ISSN 2075-1133, Inorganic Materials: Applied Research, 2020, Vol. 11, No. 1, pp. 177–180. © Pleiades Publishing, Ltd., 2020.
Russian Text © The Author(s), 2019, published in Materialovedenie, 2019, No. 7, pp. 8–11.

Features of the Ferromagnetic Resonance of Amorphous FeSiBNbCu Ribbons with Different Compositions

S. V. Komogortsev[a, c, d, *], G. S. Krainova[b], N. V. Il'in[b], V. S. Plotnikov[b], L. A. Chekanova[a], I. V. Nemtsev[a], G. Yu. Yurkin[a, d], R. S. Iskhakov[a], and D. A. Yatmanov[c]

[a] *Kirensky Institute of Physics, Krasnoyarsk Scientific Center, Siberian Branch, Russian Academy of Sciences, Krasnoyarsk, 660036 Russia*

[b] *Far Eastern Federal University, Vladivostok, 690000 Russia*

[c] *Siberian State University of Science and Technology, Krasnoyarsk, 660000 Russia*

[d] *Siberian Federal University, Krasnoyarsk, 660036 Russia*

**e-mail: komogor@iph.krasn.ru*

Received December 24, 2018; revised February 11, 2019; accepted March 19, 2019

Abstract—The resonance microwave absorption in amorphous FeSiBNbCu ribbons with different compositions obtained by rapid quenching from the melt has been investigated. It is shown that the effective magnetization calculated from the resonance field linearly decreases with increasing boron and copper impurity concentrations and the total number of nonmagnetic impurity atoms in the iron-based FeSiBNbCu ribbons.

Keywords: amorphous metal alloys, magnetic resonance, magnetic properties, magnetization

DOI: 10.1134/S2075113320010219

INTRODUCTION

The rapidly quenched FeSiBNbCu alloys are used as precursors in fractional crystallization of finemet-type materials, which are record holders among low-coercivity ferromagnetic systems [1–5]. These iron-based alloys find application in magnetic cores of high-frequency transformers, weak magnetic field sensors, and strain gauges and in magnetic screens [6–9]. The interplay of the structure and properties of such systems was investigated in many studies [10–14], but the most important questions about the high-frequency magnetization dynamics [15, 16] remain unanswered. These investigations are of great importance, since the current data processing rates require high operational speeds of elements. In addition, it is well known that the properties of amorphous alloys are determined to a great extent by their composition [10, 11, 13, 14, 17–20]; therefore, it is important to investigate the dependence of their properties upon the change in the amount of any of the components. In this study, we examine the resonance microwave absorption in amorphous FeSiBNbCu ribbons with different compositions obtained by rapid quenching from the melt.

EXPERIMENTAL

The microwave absorption curves were studied on a conventional electron spin resonance (ESR) spectrometer with a resonator pump frequency of 9.2 GHz at room temperature. The resonator type used and localization of the sample in it ensured the zero electric component of the microwave field. An external field was applied parallel to the ribbon plane. Three series of investigated ribbons had different compositions, specifically, $FeCu_{0.2}Nb_3Si_{16.5}B_6$, $FeCu_{0.5}Nb_3Si_{16.5}B_6$, and $FeCu_{1.5}Nb_3Si_{16.5}B_6$ with different copper contents; $FeCu_1Nb_5Si_{16.5}B_6$, $FeCu_1Nb_3Si_{16}B_6$, and $FeCu_1Si_{16}B_6$ with different niobium contents; and $FeCu_1Nb_3Si_{13.5}B_8$, $FeCu_1Nb_3Si_{13}B_{13}$, $FeCu_1Nb_3Si_{13.5}B_9$, $FeCu_1Nb_3Si_{13}B_6$, and $FeCu_1Nb_3Si_{14}B_5$ with different metalloid contents. The magnetization was measured on a Quantum Design MPMS SQUID magnetometer. The saturation magnetic moment was taken to be the magnetic moment in an external field of 50 kOe, which corresponded to the complete technical saturation and exceeded the coercivity by several orders of magnitude. The surface topography and ribbon thickness were controlled on a Hitachi S5500 scanning electron microscope.

RESULTS AND DISCUSSION

The differential microwave absorption spectra of the samples contain one ferromagnetic resonance (FMR) peak with different shapes and positions for different samples (Figs. 1–3). Using this peak, we determined the main characteristics of the resonance absorption, including linewidth ΔH and resonance field H_r. The ΔH and H_r values were determined by two

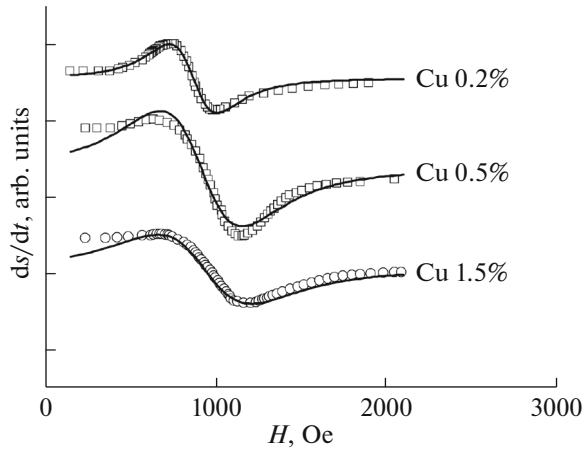

Fig. 1. Differential microwave absorption curves for the amorphous $FeCu_{0.2}Nb_3Si_{16.5}B_6$, $FeCu_{0.5}Nb_3Si_{16.5}B_6$, and $FeCu_{1.5}Nb_3Sb_{16.5}B_6$ ribbons with different copper content. The solid line shows the data fitting by the derivative of the Lorentzian function.

different approaches. In the first approach, the H_r value was calculated as the arithmetic mean between the fields of the minimum and maximum on the differential absorption curve and the ΔH value was calculated as the difference between the fields of the minimum and maximum. In the second approach, we described the experimental curves by the derivative of the Lorentzian function, where the ΔH and H_r values served as parameters providing the minimum squared deviation of the experimental data from the experiment. The resonance fields obtained by the two methods differed from each other by no more than 1–3%; therefore, hereinafter, we use only the parameters ΔH and H_r obtained by the second method (Table 1). The chosen measurement geometry allows us to use the Kittel formula for an ideal infinitely thin ferromagnetic plate (the ratio between the ribbon thickness and the measured sample length is ~0.003) to calculate the effective magnetization M_{eff} from the H_r value:

$$M_{\text{eff}} = \frac{1}{4\pi}\frac{(\omega/\gamma)^2 - H_r^2}{H_r}. \quad (1)$$

In our experiment, the ω/γ value was 2900 Oe.

The linear decrease in the effective magnetization calculated using Eq. (1) with increasing impurity concentration (Fig. 4) generally corresponds to the concept of amorphous alloys as solid solutions with unlimited solubility [1, 3]. The linear extrapolation of the data series (magnetization as a function of the total number of impurity atoms) to zero concentration yields a magnetization of about 1700 G, which is very close to the magnetization of pure bcc iron (Fig. 4). The effective magnetization includes the spontaneous magnetization and other contributions to the internal magnetic field, in particular, the induced magnetic anisotropy field and demagnetizing field, which can be caused by the surface roughness of the ribbon. Therefore, to compare three samples with different boron contents, we measured the saturation magnetization equivalent to the spontaneous magnetization of the ribbon using a vibrating sample magnetometer. According to the conventional magnetometry measurement procedure, the sample was preliminarily weighed, which allowed us to calculate the magnetization in units of G cm^3/g (emu/g). To make a comparison with the effective magnetization, we needed to estimate the magnetic moment per unit volume (G). Therefore, the thickness of some ribbons was measured also on a scanning electron microscope (Table 2), which, in turn, made it possible to estimate their density and, then, magnetization in the required units. The quantitative comparison of the M_s data from Table 2 and the M_{eff} data from Fig. 4 shows their good agree-

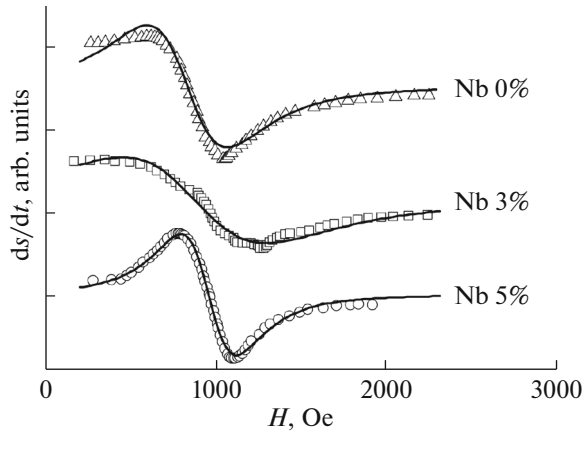

Fig. 2. Differential microwave absorption curves for the amorphous $FeCu_1Nb_5Si_{16.5}B_6$, $FeCu_{0.5}Nb_3Si_{16}B_6$, and $FeCu_1Nb_3Sb_{16}B_6$ ribbons with different niobium content.

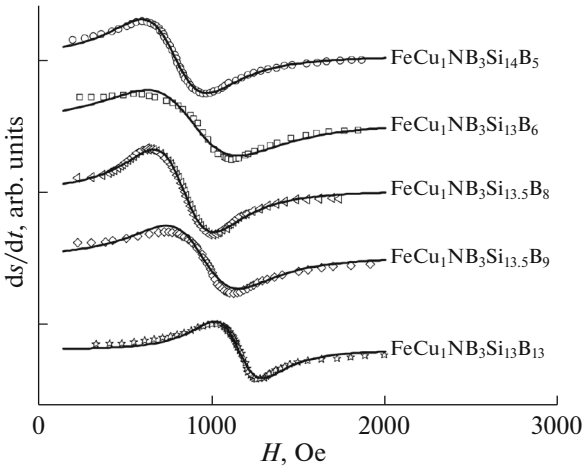

Fig. 3. Differential microwave absorption curves for the amorphous FeCuNbSiB ribbons with different metalloid content.

Table 1. Parameters of the ferromagnetic resonance of the FeCuNbSiB alloys with different compositions

Feature of the alloy series	Alloy	H_r, Oe	ΔH_{FMR}, Oe
Different copper content	$FeCu_{0.2}Nb_3Si_{16.5}B_6$	870	240
	$FeCu_{0.5}Nb_3Si_{16.5}B_6$	900	520
	$FeCu_{1.5}Nb_3Si_{16.5}B_6$	940	550
Different niobium content	$FeCu_1Si_{16}B_6$	830	420
	$FeCu_1Nb_3Si_{16}B_6$	810	920
	$FeCu_1Nb_5Si_{16.5}B_6$	950	320
Different metalloid content	$FeCu_1Nb_3Si_{14}B_5$	790	370
	$FeCu_1Nb_3Si_{13}B_6$	840	560
	$FeCu_1Nb_3Si_{13.5}B_8$	830	380
	$FeCu_1Nb_3Si_{13.5}B_9$	930	400
	$FeCu_1Nb_3Si_{13}B_{13}$	1150	220

The errors of determination of H_r and ΔH are hereinafter 20 and 10 Oe, respectively.

Table 2. Thickness and density of some FeCuNbSiB ribbons

Ribbon composition	Ribbon thickness, μm	Density, g/cm^3	M_s, G
$FeCu_1Nb_3Si_{13}B_{13}$	22.0	7.6 ± 0.4	790
$FeCu_1Nb_3Si_{13,5}B_9$	18.0	7.0 ± 0.3	750
$FeCu_1Nb_3Si_{13}B_6$	16.5	7.85 ± 0.14	850
$FeCu_1Nb_3Si_{13}B_5$	15.0	8.29 ± 0.11	—

ment. A slight (within 10%) excess of the M_s value over M_{eff} can be related to the demagnetizing fields induced by the ribbon surface roughness, which can be seen on its cross section with a scanning electron microscope.

Concerning the absorption linewidth ΔH (Table 1), no noticeable dependence of this parameter on the chemical composition of the ribbons was observed. The linewidth is fairly large and ranges from 220 to 920 Oe. The main contribution to the linewidth of the investigated ribbons is made by the so-called nonuniform broadening caused by the nonuniformity of the local parameters of a ribbon (the magnetization and magnetic anisotropy field) [15, 21–24]. This nonuniformity, in turn, can be related to both the natural fluctuations of the chemical composition and technologically induced gradients, including the stress gradient in the transverse direction of the ribbon surface. Thus, the ΔH value can be used in the comparative estimation of such inhomogeneities in different ribbons. It may be noted that the narrowest lines are observed in the alloys with the minimum copper content and the maximum boron content. It is well known that, during crystallization of the amorphous alloys of this family, copper clusters primarily form [25]. Thus, it is the copper additive that makes a decisive contribution to the development of the chemical nonuniformity of the alloy at the early stages of crystallization. The boron impurity in these alloys plays the role of a stabilizer of the nonequilibrium amorphous state; therefore, it can be expected that an increase in its concentration should lead to homogenization of the alloy, since the limiting disorder in the spatial arrangement of atoms corresponds to the highest spatial homogeneity [1, 3].

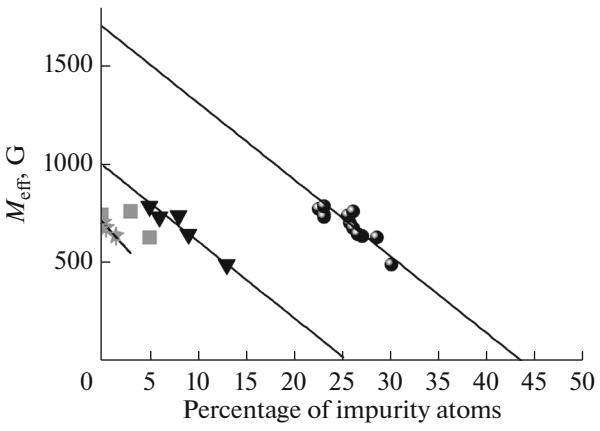

Fig. 4. Effective magnetization of the amorphous FeCuNbSiB alloys as a function of (●) the total B + Si + Nb + Cu content, (▲) B content, (□) Nb content, and (★) Cu content.

CONCLUSIONS

The linear decrease in the magnetization of the iron-based amorphous FeSiBNbCu ribbons with increasing concentration of the boron and copper impurities and the total number of impurity atoms was established using the ferromagnetic resonance method. Study of the ferromagnetic resonance linewidth points out possible ways of controlling the uniformity of the alloy upon variation in its composition.

REFERENCES

1. McHenry, M.E., Willard, M.A., and Laughlin, D.E., Amorphous and nanocrystalline materials for applications as soft magnets, *Prog. Mater. Sci.*, 1999, vol. 44, no. 4, pp. 291–433.
2. Glezer, A.M., Amorphous alloys: Past, present, and future, *Izv. Ross. Akad. Nauk, Ser. Fiz.*, 2001, vol. 65, no. 10, p. 1382.
3. O'Handley, R.C., Physics of ferromagnetic amorphous alloys, *J. Appl. Phys.*, 1987, vol. 62, no. 10, pp. R15–R49.
4. Herzer, G., Modern soft magnets: Amorphous and nanocrystalline materials, *Acta Mater.*, 2013, vol. 61, no. 3, pp. 718–734.
5. Sheftel', E.N. and Bannykh, O.A., Nanocrystalline films of soft magnetic iron-based alloys, *Russ. Metall. (Engl. Transl.)*, 2006, vol. 2006, no. 5, pp. 394–399.
6. Rodionova, V., et al., The stress components effect on the Fe-based microwires magnetostatic and magnetostrictive properties, *J. Magn. Magn. Mater.*, 2017, vol. 422, pp. 216–220.
7. Zhukova, V., et al., Tailoring of magnetoimpedance effect and magnetic softness of Fe-rich glass-coated microwires by stress-annealing, *Sci. Rep.*, 2018, vol. 8, no. 1, pp. 3202.
8. Kurlyandskaya, G.V., Giant magnetoimpedance for biosensing: Advantages and shortcomings, *J. Magn. Magn. Mater.*, 2009, vol. 321, no. 7, pp. 659–662.
9. Antonov, A.S. and Buznikov, N.A., Asymmetry in the nonlinear magneto-impedance of an amorphous microwire in the presence of a magnetizing current, *Materialovedenie*, 2016, no. 1, pp. 3–9.
10. Yoshizawa, Y. and Yamauchi, K., Magnetic properties of Fe–Cu–M–Si–B (M = Cr, V, Mo, Nb, Ta, W) alloys, *Mater. Sci. Eng., A*, 1991, vol. 133, pp. 176–179.
11. Mushnikov, N.V., et al., Magnetic properties and structure of nanocrystalline FINEMET alloys with various iron contents, *Phys. Met. Metallogr.*, 2015, vol. 116, no. 7, pp. 663–670.
12. Herzer, G., Soft magnetic nanocrystalline materials, *Scr. Metall. Mater.*, 1995, vol. 33, no. 10–11, pp. 1741–1756.
13. Menushenkov, V.P., et al., Investigation of the structure and magnetic properties of metastable phases in Fe–B alloys melt spun, *Inorg. Mater.: Appl. Res.*, 2016, vol. 7, no. 1, pp. 40–44.
14. Sheftel', E.N., et al., Phase-structure state of Fe–Zr–N magnetic films produced by magnetron sputtering of heated target, *Materialovedenie*, 2014, no. 10, pp. 8–14.
15. Komogortsev, S.V., et al., Properties of ferromagnetic resonance in $Fe_{73.5}CuNb_3Si_{13.5}B_9$ nanocrystalline alloys, *Phys. Solid State*, 2010, vol. 52, no. 11, pp. 2287–2290.
16. Rubinstein, M., Harris, V.G., and Lubitz, P., Ferromagnetic resonance in nanocrystalline $Fe_{73.5}CuNb_3Si_{13.5}B_9$ (Finemet), *J. Magn. Magn. Mater.*, 2001, vol. 234, no. 2, pp. 306–312.
17. Kotvitskii, A.N., et al., Effect of annealing on the magnetic characteristics of iron-based spinning tapes, *Izv. Ross. Akad. Nauk, Ser. Fiz.*, 2015, vol. 79, no. 6, pp. 795–799.
18. Ilin, N.V., et al., Effect of composition on the structural relaxation of amorphous iron-based alloys, *Bull. Russ. Acad. Sci., Phys.*, 2017, vol. 81, no. 3, pp. 387–390.
19. Kraynova, G., et al., Features of magnetic state of Fe-based melt-spun alloys upon heating, *Proc. 2015 IEEE International Magnetics Conference (INTERMAG)*, Piscataway, NJ: Inst. Electr. Electron. Eng., 2015, art. ID 7157527.
20. Kotvitckii, A.N., et al., Changes in the magnetic parameters of amorphous alloys as an indicator of structural transformations, *Bull. Russ. Acad. Sci., Phys.*, 2013, vol. 77, no. 10, pp. 1206–1209.
21. Sheftel, E.N., et al., Investigation of the magnetic properties and magnetic structure parameters of nanocrystalline $Fe_{79}Zr_{10}N_{11}$ films, *Bull. Russ. Acad. Sci., Phys.*, 2010, vol. 74, no. 10, pp. 1449–1451.
22. Sidorenko, P.K., Sheftel', E.N., and Komogortsev, S.V., The magnetic properties and parameters of the magnetic structure of nanocrystalline $Fe_{79}Zr_{10}N_{11}$ films, *Perspekt. Mater.*, 2010, no. 9, pp. 224–227.
23. Iskhakov, R.S., Denisova, E.A., Komogortsev, S.V., Chekanova, L.A., Kalinin, Yu.E., and Sitnikov, A.V., Ferromagnetic resonance and magnetic microstructure in nanocomposite films of $Co_x(SiO_2)_{1-x}$ and $(CoFeB)_x(SiO_2)_{1-x}$, *Phys. Solid State*, 2010, vol. 52, no. 11, pp. 2263–2266.
24. Komogortsev, S.V., et al., Random magnetic anisotropy and ferromagnetic resonance in nanosrystalline alloy Fe73.5CuNb3Si13.5B9, *Solid State Phenom.*, 2011, vol. 168–169, pp. 365–368.
25. Hono, K., et al., Microstructures of $Fe_{73.5}Si_{13.5}B_9Nb_3Cu_1$ nanocrystalline soft magnetic material investigated by APFIM and HRTEM, *Surf. Sci.*, 1992, vol. 266, nos. 1–3, pp. 385–390.

Translated by E. Bondareva